Accepted Manuscript

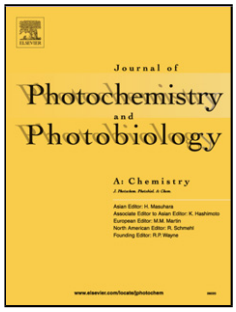

Title: Photophysics, photochemistry and thermally-induced redox reactions of a (Pterin)rhenium(I) complex

Authors: Fabricio Ragone, Pedro David Gara, Fernando S.García Einschlag, Alexander G. Lappin, Guillermo J. Ferraudi, Ezequiel Wolcan, Gustavo T. Ruiz

PII: S1010-6030(17)31550-2
DOI: https://doi.org/10.1016/j.jphotochem.2018.02.015
Reference: JPC 11146

To appear in: *Journal of Photochemistry and Photobiology A: Chemistry*

Received date: 24-10-2017
Revised date: 2-1-2018
Accepted date: 10-2-2018

Please cite this article as: Fabricio Ragone, Pedro David Gara, Fernando S.García Einschlag, Alexander G.Lappin, Guillermo J.Ferraudi, Ezequiel Wolcan, Gustavo T.Ruiz, Photophysics, photochemistry and thermally-induced redox reactions of a (Pterin)rhenium(I) complex, Journal of Photochemistry and Photobiology A: Chemistry https://doi.org/10.1016/j.jphotochem.2018.02.015

Photophysics, photochemistry and thermally-induced redox reactions of a (Pterin)rhenium(I) complex

Fabricio Ragone[1], Pedro David Gara[2], Fernando S. García Einschlag[1], Alexander G. Lappin[3], Guillermo J. Ferraudi[4], Ezequiel Wolcan[1,*] and Gustavo T. Ruiz[1,*]

[1] *Instituto de Investigaciones Fisicoquímicas Teóricas y Aplicadas (INIFTA, UNLP, CCT La Plata-CONICET), Diag. 113 y 64, C.C. 16 Sucursal 4, B1906ZAA, La Plata, Argentina. Email:* gruiz@inifta.unlp.edu.ar; ewolcan@inifta.unlp.edu.ar

[2]*Centro de Investigaciones Ópticas (CIOp, CONICET-CIC) and UNLP, C.C. 3 (1897), La Plata, Argentina*

[3]*Department of Chemistry and Biochemistry, Univ. of Notre Dame, Notre Dame, IN 46556, United States*

[4]*Radiation Research Building, Univ. of Notre Dame, Notre Dame, IN 46556, United States*

Graphical abstract

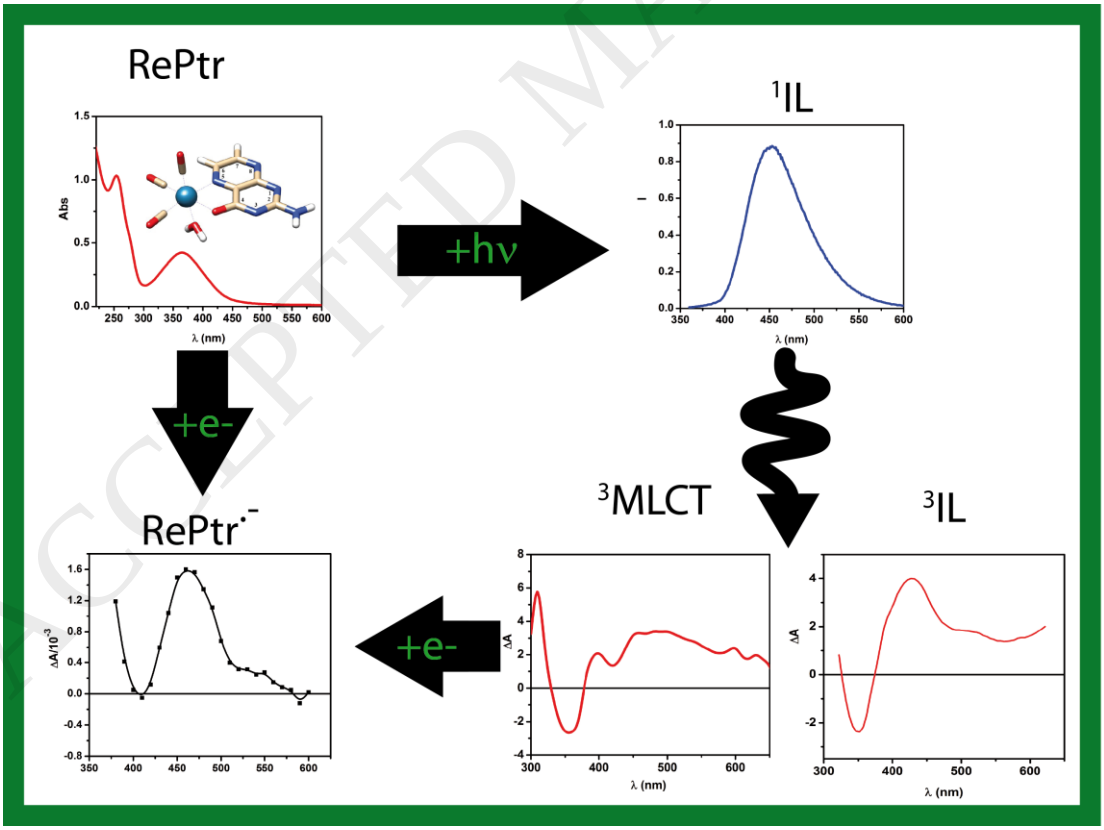

Highlights

- Photophysics and photochemistry study of the (Pterin)rhenium(I) complex
- Nature of the excited states depend on solvent polarity.
- Flash photolysis and Pulse radiolysis experiments generated reactive species
- MCR-ALS analysis and TD-DFT calculations helped to ascertain the nature of these species

Abstract

In this work, we present a whole and deep study on the thermal redox and the photophysical and photochemical reactions of a tricarbonyl Re(I) complex coordinating Pterin, *fac*-$Re^{I}(CO)_3$(pterin)(H_2O) (pterin = 2-amino-4-oxo-3H-pteridine)**.** In aqueous solutions, the fluorescence of the complex is attributed to the emitting ^{1}IL state (τ_{emi} ~ 7.6 ns). In MeCN, however, the luminescence was ascribed to an overlapping dual emission from ^{1}IL and ^{3}MLCT states (τ_{emi1} = 8.0 ns and τ_{emi2} = 1.0 μs). Oxygen quenching of the ^{3}MLCT based luminescence occurred with k_q = 1.6 x 10^9 $M^{-1}s^{-1}$. In glasses at 77K, nevertheless, the ^{3}MLCT prevailed over ^{1}IL states. Flash photolysis experiments in aqueous solutions showed the spectrum of ^{3}IL while in MeCN the presence of ^{3}MLCT was evident. Pulse radiolysis experiments under oxidizing and reducing environments were performed in aqueous solutions of the Re-Pterin complex. By performing multivariate curve resolution - alternating least-squares (MCR-ALS), two species were identified under reducing conditions: an intermediate related to the semireduced radical of pterin ligand and the dihydrogenated [$Re(CO)_3$(7,8-$PtrH_2$)(H_2O)] product. TD-DFT calculations helped to ascertain the nature of these species. Flash photolysis experiments where the excited states were reduced with triethylamine were in good agreement with pulse radiolysis

experiments under reductive conditions. The oxidized transient spectrum was also obtained by pulse radiolysis, which compares very well with those published for Re(II) species, leading us to propose oxidation in the metal core as the reaction product of the transient under oxidizing conditions.

The combination of different spectroscopic techniques along with the theoretical calculation allowed elucidating the nature, dynamics and reactivity of the excited states prevail in a Re-Pterin complex. This is of the particular importance considering that equivalent studies have not been reported for any other rhenium complex of substituted pterins nor for complexes of other transition metal ions of pterin derivatives.

KEYWORDS

Rhenium complex, photochemistry, excited states, Pterin, TD-DFT.

Introduction

Pterins (2-amino-4-oxo-3H-pteridine) (Ptr) are heterocyclic compounds widely distributed in biological systems. Pterins are involved in various photobiological processes, in the mammal metabolically routes, in sensory organs of vertebrates and invertebrates and pigments in arthropods [1],[2]. The photochemical and photophysical properties of pterins have been extensively studied [3]–[7]. The coordination of an organic ligand to a metal introduces new electronic transitions such as metal-to-ligand charge transfers (MLCTs). These MLCT excited states show a strong dependence on the polarity of the solvent and a

marked heavy metal effect, the latter being reflected in quantum yields of triplet formation close to unity [8].

Transition metal complexes comprise an interesting and widely extended field for studies related to different areas of scientific research such as electron transfer studies [9], solar energy conversion [10], and catalysis [11]. Possible applications as luminescent sensors [12],[13] and molecular materials for nonlinear optics or optical switching [14],[15] have also emerged. In particular, luminescent transition metal complexes of Re(I) and Ru(II) with polypyridyl ligands have been recognized as good potential candidates for the development of pH sensing devices [16],[17] (and references therein). Moreover, there are potential biochemical and technical applications based on the formation of adducts between transition metal complexes of Re(I), Ru(II), Os(III), Rh(III), or Co(III) and biological macromolecules such as DNA which take advantage of the luminescent properties of the ^{3}MLCT states [18]–[20]. As these complexes show exceptionally rich excited-state behavior and redox chemistry as well as thermal and photochemical stability [8] they have also been used as biological labelling reagents and noncovalent probes for biomolecules and ions [13]. In this regard, some complexes including biologically relevant ligands, such as substituted pterins, coordinated to the $Re(CO)_3Cl$ core have been synthesized and characterized [21]–[23].

As far as we know, there are only a few examples concerning the photophysical properties of metallic complexes coordinating pterin and at present there are not published papers in the literature regarding the photophysical properties of Re(I) complexes that coordinate that ligand [24]. In this work, we present a whole and deep study on the solvent

dependent thermal redox and the photophysycal and photochemical reactions of a tricarbonyl Re(I) complex coordinating Ptr, *fac*-$Re^{I}(CO)_3$(pterin)(H_2O) (**RePtr**).

Experimental Part

Materials.

The **RePtr** complex was available from previous work [25][26]. Spectrograde and HPLC grade acetonitrile (MeCN) (J.T. Baker), methanol (MeOH, Sigma Aldrich) and ethanol (EtOH, Sigma Aldrich) were used without further purification. 2-hydroxybenzophenone, phenalenone, New Coccine, D_2O, NaOH, and $HClO_4$ were purchased from Sigma Aldrich at the highest purity available and were used as received. Deionized water (> 18 MΩ cm^{-1}, < 20 ppb of organic carbon) was obtained with a Millipore system.

Photophysical Measurements.

UV-vis spectra were recorded on a Shimadzu UV-1800 spectrophotometer. Emission spectra were obtained with a computer-interfaced Near-IR Fluorolog-3 Research Spectrofluorometer, and were corrected for differences in spectral response and light scattering. Solutions were deaereated with ultrahigh-purity O_2-free nitrogen in a gas-tight apparatus before recording the spectra.

Emission quantum yields, ϕ_{em}, were calculated with **eq. 1**, by using solutions of a reference compound with a known quantum yield of emission, ϕ_{ref}

$$\phi_{em} = \left(\frac{A_{ref}}{A_s}\right)\left(\frac{I_s}{I_{ref}}\right)\left(\frac{n_s}{n_{ref}}\right)^2 \phi_{ref} \qquad \textbf{(1)}$$

In **eq. 1**, n_s and n_{ref} are the refractive indexes of the solutions containing the sample and the reference compound respectively, *A* is the absorbance of the sample or reference at the excitation wavelength (A_s and A_{ref} < 0.1) and I is the integral of the emission spectrum and was used as a relative measure of the respective intensities of the luminescence. An aqueous solution of pterin at pH=5 was used as a reference with ϕ_{ref} = 0.33 [27]. Emission lifetime measurements were performed using either Fluorolog-3 with Time-correlated Single-Photon Counting (TCSPC) unit with either 341 and/or 388 nm NanoLEDs. Photoacoustic measurements were performed by using a set-up already described [28]. The resolution time in our experimental set-up, τ_R, was ca. 800 ns [28]. New Coccine or 2-hydroxybenzophenone were used as calorimetric reference (CR) compounds in the buffer and in MeCN solutions, respectively [29][30]. Experiments were performed under a controlled atmosphere, bubbling N_2 or O_2 in the solution, for 15 min. In principle, all the excited species with lifetimes $\tau \leq {}^1/_5\,\tau_R$ release their heat content as prompt heat, whereas excited species with a lifetime of $\tau \geq 5\,\tau_R$ function as heat storage within the time resolution of the LIOAS experiment.

For the handling of the LIOAS signals, **eq. 2** was used, which relates the peak to peak amplitude of the first optoacoustic signal (*H*) with the fraction of the excitation laser fluence (*F*) absorbed by the sample [31].

$H = K\,\alpha\,F\,(1\text{-}10^{-A})$ **(2)**

In this equation the experimental constant *K* contains the thermo-elastic parameters of the solution as well as instrumental factors, *A* is the absorbance of the sample at λ_{exc} and α is the fraction of the energy released to the medium as prompt heat, i.e. within the time resolution of the experiment.

The efficiency of **RePtr** complex toward singlet oxygen sensitization was assessed by the direct measurement of the $^1O_2$ ($^1\Delta_g$) near-infrared luminescence. After the irradiation of aerated solutions of the complex the generation of $^1O_2$ ($^1\Delta_g$) was evidenced by the appearance of the characteristic $^1O_2$ ($^1\Delta_g$) $\rightarrow$ $^3O_2$ phosphorescence at 1270 nm. Time resolved phosphorescence detection was used for singlet oxygen detection. The near IR luminescence of $^1O_2$ ($^1\Delta_g$) was detected by Ge-photodiode (Applied Detector Corporation, time resolution 1 µs). The quantum yield of $^1O_2$ ($^1\Delta_g$) formation, ϕ_Δ, was determined by measuring its phosphorescence intensity using an optically matched solution of phenalenone (ϕ_Δ = 0.98) [32] as a reference sensitizer.

Transient absorption spectra were recorded using flash photolysis apparatus described elsewhere [33]. In these experiments, 25 ns flashes of 351nm (ca. 25-30 mJ/pulse) light were generated with a Lambda Physik SLL-200 excimer laser. Decays typically represented the average of 10 to 30 pulses. Edinburgh L980 flash photolysis instrument with Nd:YAG laser Continum (355 nm, laser pulse ~30 ns) excitation sources was also used. The intensity of both emitted and scattered light was subtracted in each trace. Solutions for the photochemical work were deoxygenated with streams of ultrahigh-purity N_2 before

and during the irradiations. A flow system ensured that the fresh solution was brought to the reaction cell in experiments where the decomposition of the Re(I) complexes and/or formation of products interfered with the optical measurements. The concentration of the complexes were adjusted to provide homogeneous concentrations of the photogenerated intermediates within the volume of the irradiated solution, *i.e.,* optical densities equal to or less than 0.1 (optical length = 1 cm) at 355 nm.

Curve Resolution Methods

For the analysis of the time-resolved difference spectra we have chosen one of the most widely used algorithms namely multivariate curve resolution - alternating least-squares (MCR-ALS), which can provide simultaneous estimates for the concentration and spectral profiles of unknown spectroscopic mixtures [34],[35] (and references therein).

Pulse radiolysis

Pulse radiolysis experiments were carried out with a model TB-8/16-1S electron linear accelerator. The instrument and computerized data collection for time-resolved UV-vis spectroscopy and reaction kinetics have been described elsewhere [36],[37].

In the several ns time domain, the radiolysis of H_2O, eq. 3, yields e^-_{aq}, H and $^\bullet$OH radicals [38]:

$$H_2O \rightsquigarrow e^-_{aq}, {}^\bullet OH, H, H^+ \qquad \textbf{(3)}$$

The hydrated electron, the strongest chemical reductant (-2.8 V *vs.* NHE), will often reduce a substrate S to $S^{\bullet-}$ in a diffusion-controlled reaction, eq. 4:

$S + e^-_{aq} \rightarrow S^{\bullet-}$ **(4)**

The oxidizing $^{\bullet}OH$ radical can efficiently be removed to prevent its reaction with S by the addition of tert-butyl alcohol or 2-propanol, eqs. 5-6 [38]:

$^{\bullet}OH + (CH_3)_3COH \rightarrow H_2O + (^{\bullet}CH_2)C(CH_3)_2OH$ **(5)**

$^{\bullet}OH + (CH_3)_2CHOH \rightarrow H_2O + (CH_3)_2C^{\bullet}OH$ **(6)**

The $(CH_3)_2C^{\bullet}OH$ radical, being a more powerful reducing radical (E^0 = -1.2 V vs NHE) than the $(^{\bullet}CH_2)C(CH_3)_2OH$ radical (E^0 = -0.1V vs NHE), will usually reduce S to $S^{\bullet-}$ (eq. 7)

$S + (CH_3)_2C^{\bullet}OH \rightarrow S^{\bullet-} + H^+ + (CH_3)_2CO$ **(7)**

However, the $(^{\bullet}CH_2)C(CH_3)_2OH$ radical in some occasions may also yield $S^{\bullet-}$.

Other $^{\bullet}OH$ radical scavenger is formate, HCO_2^-. The $CO_2^{\bullet-}$ formed radical from eq. 8 will generally yield the same $S^{\bullet-}$ via eq. 9 [38]:

$^{\bullet}OH + HCO_2^- \rightarrow H_2O + CO_2^{\bullet-}$ **(8)**

$S + CO_2^{\bullet-} \rightarrow S^{\bullet-} + CO_2$ **(9)**

Since $^{\bullet}OH$ radical is an oxidizing species which reacts with a lack of selectivity, it may be converted to more selective oxidizing radicals like $X_2^{\bullet-}$ (X = halogen or SCN^-) and $N_3^{\bullet}$, eqs. 10-11, when it is needed to study thermal oxidations of S by pulse radiolysis experiments [38].

$^{\bullet}OH + 2X^- \rightarrow X_2^{\bullet-} + OH^-$ **(10)**

$^{\bullet}OH + N_3^- \rightarrow N_3^{\bullet} + OH^-$ **(11)**

In the study of oxidations reaction 4 is unwanted. It is simple to remove the reducing radical e^-_{aq} after the saturation of the solution with N_2O, eq. 12 [38].

e^-_{aq} + N_2O + $H_2O \rightarrow {}^{\bullet}OH + OH^- + N_2$ **(12)**

Thiocyanate dosimetry was carried out at the beginning of each experimental session. Details of the dosimetry have been reported elsewhere [37],[39]. The procedure is based on the concentration of $(SCN)_2^{\bullet-}$ radicals generated by the electron pulse in a N_2O-saturated 10^{-2} M SCN^- solution (eq. 10). In the procedure, the calculations were made with G = 6.13 and an absorption coefficient $\varepsilon = 7.58 \times 10^3\ M^{-1}\ cm^{-1}$ at 472 nm [37],[39] for the $(SCN)_2^{\bullet-}$ radicals**.** In general, the experiments were carried out with doses that in N_2-saturated aqueous solutions resulted in $(1.7\pm0.1) \times 10^{-6}$ M to $(6.0\pm0.3) \times 10^{-6}$ M concentrations of e^-_{aq}. In these experiments, solutions were deaerated with streams of N_2 or N_2O gasses. In order to irradiate a fresh sample with each pulse, an appropriate flow of the solution through the reaction cell was maintained during the experiment.

Computational details

The electronic structure of the rhenium complex was studied by performing Density Functional Theory [40]–[42] (DFT) and Time Dependent Density Functional Theory (TD-DFT) [43]–[45] (TD-DFT) calculations using Gussian 09 software [46]. The ground state structure of the complex was optimized by DFT calculations using B3LYP functional and LanL2DZ basis set. Vibrational frequencies were computed at the same level of theory to confirm that these structures were minima on the energy surfaces. Solvents effects (H_2O) on the optimization of the ground state structure were taken into account by means of the Polarizable Continuum Model (PCM) [47]–[49]. At the optimized ground state geometries, a set of 200 vertical excitations were computed with the PBE0 hybrid

functional in H_2O. The PBE0 hybrid functional was shown to give a very good performance in the simulation of the electronic spectrum of $Re(CO)_3(Ptr)(H_2O)$ as evidenced by the best match (relative to the performance of other functionals as B3LYP, XB3LYP and CAM-B3LYP) between calculated and experimental electronic transitions [7]. Therefore, all the electronic transitions presented hereafter are those calculated using PBE0 functional for the Re(I) complex. TD-DFT calculations with the PBE0 functional were performed using the 6-311++G(d,p) basis set for C, N, O and H atoms while LanL2TZ(f) [50],[51] (triple zeta basis set designed for an ECP plus f polarization) was used for Re atom. Absorption spectra were simulated with Gaussian distributions with a full-width at half-maximum (fwhm) set to 3000 cm^{-1} with the aid of GaussSum 2.2.5 program [52]. The calculated electronic spectra of $Re(CO)_3(Ptr)(H_2O)$ are simulated from the theoretical results to ease the comparison with experimental data.

Results and discussion

Photophysical Processes

The luminescence spectrum of **RePtr** in air-equilibrated aqueous solutions upon excitation in the low energy band (λ_{exc} = 350 nm) consists of a broad unstructured band with λ_{max} centered around 450 nm. When the aqueous solutions were deaerated by bubbling either O_2-free N_2 or O_2 no significant differences were observed either in λ_{max}, ϕ_{em} and/or luminescence lifetime (τ_{em}). In acidic solutions (pH = 3 and pH = 6) the emission band is centered at λ_{max} = 441 nm while in alkaline solutions (pH = 10) the luminescence maximum

experiences a bathochromic shift to λ_{max} = 454 nm, see **Figure 1**. In previous work [25], protonation studies in aqueous solutions of the RePtr complex showed two acid-base equilibriums with pK_{a1} = 3.9 and pK_{a2} = 8.8. pK_{a1} was assigned to the protonation equilibrium at N3, see **Figure S1**, of the pterin ligand in the complex and pK_{a2} could be ascribed to the deprotonation of a coordinated water molecule. Therefore, the species present are $[Re(CO)_3(Ptr)(OH)]^-$ (**RePtr$^-$**) at pH = 10 and $[Re(CO)_3(Ptr)(H_2O)]$ and $[Re(CO)_3(PtrH)(H_2O)]^+$ (**RePtr$^+$**) at pH = 6 and pH = 3, respectively. Nevertheless, neither spectral shifts nor band shape differences can be observed from the comparison of the luminescence spectra of **RePtr** complex at both acidic pHs. The emission quantum yield, however, increases moderately from 6.4 x 10^{-2} at pH = 3 to 9.1 x 10^{-2} at pH = 6 while at pH = 10 it experiences a dramatic enhancement to ϕ_{em} = 0.25. Conversely, the luminescence decays, which are monoexponential with lifetimes around 7 ns, experience only minor changes upon pH change (See Table 1).

The luminescence parameters of **RePtr** complex in alkaline media shows similar characteristics to the fluorescence of the free ligand at pH = 10.5, i.e., both λ_{max} and ϕ_{em} are similar [6]. On the other hand, the emission quantum yield of **RePtr** complex in acidic media is one order of magnitude smaller than that of the Ptr ligand. After irradiation of the **RePtr** complex at λ_{exc} = 350 nm in aqueous solution, the ^{1}IL and ^{1}MLCT excited states are simultaneously populated. These excited states later populate via intersystem crossing processes, ISC, the respective ^{3}IL and ^{3}MLCT. Population of the latter is favored by the strong spin-orbit coupling induced by the metal ion in the complex. TD-DFT predicts that

the low energy absorption band of both **RePtr** and **RePtr**$^-$ consist of a H-1→L transition [7]. **Figure S2** shows density of states (DOS) plot for those rhenium species. It is observed that H-1→L transition in **RePtr** has a marked MLCT ($Re(CO)_3$→Ptr) character while in **RePtr**$^-$ that transition has, in addition, a considerable IL Ptr ($\pi \rightarrow \pi^*$) character. Since population of MLCT is more important than population of IL states, a lower luminescence quantum yield is expected for **RePtr** than pterin. On the other hand, when the prevalent specie is **RePtr**$^-$ (basic solution) the contribution of MLCT to the overall excited state is less important prevailing the IL character, and as consequence, the luminescence quantum yield of **RePtr** complex is similar to that of free pterin.

Luminescence properties were also determined in acetonitrile solutions of **RePtr** complex, **Figure 2**. In that condition, we can assume that the coordinated water molecule is replaced by one acetonitrile molecule being the $[Re(CO)_3(Ptr)(MeCN)]$ complex the prevalent species in this solvent [53].

Two emission bands were observed in the luminescence spectrum of **RePtr** complex upon excitation with λ_{exc} = 350 nm in acetonitrile. The most intense emission band at λ_{max} = 418 nm is nearly 30 nm blue shifted relative to the emission in aqueous solutions. The emission band centered at λ_{max} ~ 570 nm has a lesser intensity than the band at λ_{max} = 418 nm and it is quenched by the presence of oxygen in the solution, **Figure 2B**. When the excitation wavelength is λ_{exc} = 400 nm the low energy band is clearly observed while the luminescence band centered at λ_{max} = 418 nm decreased in intensity, **Figure S3A**. In MeOH/EtOH glasses at 77 K, the high energy band has almost disappeared and only a luminescence peaking at 575 nm is observed, **Figure S3B**.

The same luminescence centered at 418 nm is observed with the **RePtr** complex and the free pterin in MeCN, pointing to the IL character of this emission. However, the additional feature centered at 570 nm, present in the luminescence of the **RePtr** complex, is not observed in acetonitrile solution of free pterin, **Figure S4**.

A sum of two exponentials was required to achieve a satisfactory fit of the emission decay profiles from acetonitrile solutions of **RePtr** complex at λ_{em} = 570 nm. The fast component decay is τ = 8.0 ns under N_2 atmosphere and it is insensitive to the presence of oxygen in the solution. On the other hand, the slow component decay is τ = 1.0 μs under N_2 atmosphere and it was shortened by the presence of molecular oxygen, Table 1. The bimolecular rate constant for the quenching of the **RePtr** complex luminescence by oxygen (k_q, Table 1) has been determined from the slope of the linear Stern-Volmer plot ($\tau_0/\tau = 1 + k_q\tau_0[O_2]$) calculated with the values of the emission lifetimes in the absence and in the presence of oxygen (τ_0 in N_2 and τ in air and in O_2, respectively). The oxygen solubility at 1.013 bar of air was calculated according to $[O_2] = 0.21(P_A\text{-}P_v)[O_2]_{P=1}$ [54], where P_A and P_v are the atmospheric pressure and the vapor pressure of the solvent, respectively and $[O_2]_{P=1}$ is the oxygen concentration in the solvent at a 1.013 bar partial pressure of O_2. The saturated oxygen solubility at 1.013 bar in the organic solvents and water were taken from literature values [28],[55]. A bimolecular rate constant of k_q = 1.6 x 10^9 $M^{-1}s^{-1}$ was calculated from the Stern-Volmer plot., **Figure S5**.

Singlet oxygen generation by the **RePtr** complex in both D_2O (at pD 4, 6 and 10) and MeCN solutions was analyzed by time resolved phosphorescence measurements (1270 nm). The phosphorescence of acetonitrile solutions showed clear evidence of singlet oxygen

formation. Nevertheless, singlet oxygen generation in D_2O solutions could not be detected under our experimental conditions. Linear correlations were obtained from the plots of the dependence of the singlet oxygen phosphorescence intensity emission at zero time, S(0), as a function of the laser energy for the complex and the reference. From these slopes (**Figure S6**) and the usual procedure described elsewhere [30],[56] the determined quantum yield of $O_2(^1\Delta_g)$ production was $\Phi_\Delta = 0.06$ in MeCN and $\Phi_\Delta < 10^{-3}$ in D_2O. LIOAS experiments carried out with both acetonitrile and aqueous solutions of Re-Ptr complex showed the same behavior: no time shift or changes of shape of the photoacoustic signal occurred with respect to the calorimetric reference (CR) signal (Inset of **Figure 3**). Linear relationships in both solvents were obtained between the amplitude of the first optoacoustic signal (*H*) and the excitation fluence (*F*) for samples and references at various *A,* in a fluence range between 1 and 20 J/m^2. The ratio between the slopes of these lines for sample and reference yielded the values of α for the samples. For the complex in MeCN solution the slopes were independent on the specific atmosphere and were the same that the CR measured at the equal experimental conditions, **Figure 3**. From these plots, considering that $\alpha_R = 1$ for CR, the α values were calculated for the **RePtr** complex in both solvents. Therefore, a value of $\alpha = 1.00 \pm 0.04$ was obtained in aqueous and in MeCN solutions (either under N_2 or O_2 atmosphere). Consequently, this complex released to the medium all the absorbed energy as prompt heat (integrated by the transducer) in processes faster than $\tau_R/5$. These values combined with fluorescence data and singlet oxygen quantum yield production fit the energy balance [28],[31].

Photochemical Reactions.

Figure 4 shows the absorption spectra of the transient generated when deaerated aqueous solutions of **RePtr** ([Re]=1 x 10^{-4} M at pH=6) were irradiated at 355 nm in flash photolysis experiments. An absorption maximum near 430 nm overlapped with another band at 400 nm and a long tail stretching up to λ ~ 650 nm were observed. The ground state depletion in the 300-400 nm region and the presence of isosbestic points makes it possible to determine ε_T (330 nm) = 2100 and ε_T (370 nm) = 4600 $M^{-1}cm^{-1}$ (ε_T = absorption coefficient of transient)**.** A 430 nm trace could be fitted by a mono-exponential function with a lifetime τ_T ~ 2 μs, Figure S7. Since the transient spectra bear a strong resemblance with those of the pterin triplet [57][4], the transient spectra can be assigned to the IL triplet excited state in the **RePtr** complex decaying by radiationless processes, **Figure 4**.

When 2 x 10^{-4} M solutions of **RePtr** complex in MeCN were flash irradiated at 355 nm, the generated transient shows an absorption spectrum with maximum near 400 nm, a broad absorption band spanning from 420 to 650 nm and ground state depletion in the 300-400 nm region, **Figure 5a**. **Figure 5b** shows a representative oscilographic trace of the transient at λ_{obs} = 560 nm, which could be well fitted by a mono-exponential function with a lifetime of τ_T = 1.0 μs.

The transient spectrum obtained in acetonitrile medium can be assigned as a MLCT triplet excited state based on a couple of characteristics: *i.* the spectral features which differ from that one obtained in aqueous solutions (Figure 4) and *ii*. the transient lifetime is the same to that of the slow component of the luminescence decay, i.e. $\tau_T = \tau_{emi}$ (Table 1)

Flash photolysis experiments were carried out also in the presence of the sacrificial donor triethylamine, TEA 0.1 M, under similar experimental conditions to those described in **Figure 5**. The excited state of **RePtr** reacted with TEA within the laser flash pulse to yield a transient whose spectral features, λ_{max} = 460 nm, **Figure 6A**, were different from those of the spectra in **Figure 5**. In addition, this transient decays whit τ_T = 132 μs, Figure **6B.** The nature and lifetime of this transient, generated by reaction between ^{3}MLCT excited state of **RePt**r and an electron donor as TEA, can be assigned to a reduced radical of the complex.

Flash photolysis experiments of free pterin solutions in the presence of a sacrificial reductant like guanosine have shown the generation of the reduced Ptr radical [4]. The similarity between the spectrra of **Figure 6** and that of the semireduced pterin radical is consistent with the assigment of a reduced radical in the **RePt**r complex to the transient obtained in our experimental conditions.

Pulse Radiolysis

Pulse Radiolysis (PR) experiments were carried out with **RePtr** solutions under five different experimental conditions: N_3Na/N_2O; $NaHCO_2/N_2$; $NaHCO_2/N_2O$, 2-propanol/N_2 and 2-propanol/N_2O.

Oxidation of RePtr by the $N_3^{\bullet-}$ radical

Transient spectra were recorded when a deaerated **RePtr** solution ([Re] = 4.0 x 10^{-5} M in H_2O) reacted with the pulse radiolysis generated $N_3^{\bullet-}$ radical according to eqs. 9, 10. The

transient spectrum, **Figure 7**, shows absorption bands at 340 nm and 430 nm with a shoulder at 470 nm and other less intense absorption bands between 550 and 680 nm. Because of the transient spectral shape, the oxidized product can be assigned to a **Re(II)Ptr** species [58].

Reduction of RePtr by e^-_{aq}, $(CH_3)_2C^{\bullet}OH$ and $CO_2^{\bullet-}$ radicals

The reactions of e^-_{aq}, $(CH_3)_2C^{\bullet}OH$ and/or $CO_2^{\bullet-}$ radicals, eqs. 4, 7 and 9, with **RePtr** were studied in aqueous solutions of the complex ([RePtr] = 1.78 x 10^{-5} M at pH = 6, phosphate buffer) by means of the UV-Vis spectroscopic changes. In N_2 deaerated solutions, the reaction between e^-_{aq} and the **RePtr** complex was completed within the first μs after the radiolytic pulse. The transient spectrum generated by reaction with e^-_{aq}, exhibited bands at λ_{max} ~ 375 nm and 450 nm, **Figure 8A**. It evolved to the final product in the ms time scale. A bleach of the solution at ~ 380 nm can be observed in the spectrum of the product. The same spectral features were observed in the reaction of the complex with $CO_2^{\bullet-}$ **(Figure 8B**) and $(CH_3)_2C^{\bullet}OH$ radicals (**Figure S8**). Compared to the e^-_{aq} reaction, the pseudo first order rate constants for the build-up of the intermediates generated by the C-centered radicals are an order of magnitude smaller than the case of the reduction with e^-_{aq} (see below).

Analyses of the time resolved spectra.

The SVD and MCR-ALS methods were used for the analyses of the time-resolved difference spectra of pulse radiolysis experiments. Three contributions were required to explain with accuracy the trends observed in the spectra generated with each radical. In the fitting procedure non-negative and closure constraints were used. The individual contributions resolved by MCR-ALS method, which allow explaining the entire set of time resolved difference spectra recorded for the experiments performed in the presence of formate/N_2 or /N_2O, are given as supplementary material (**Figure S9**). The spectral contribution labeled as Sp1 (N_2) was ascribed to the solvated electron, $\boldsymbol{e}^{-}_{aq}$, whereas the contribution labeled as Sp1 (N_2O) was assigned to the carbon dioxide anion radical, $CO_2^{\bullet-}$. Similar results were obtained for Sp1 (N_2, N_2O) in the presence of 2-propanol.

On the other hand, the other two spectral contributions, labeled in **Figure S9** as Sp2 (N_2)/Sp2 (N_2O) and Sp3 (N_2)/Sp3 (N_2O), were independent of the experimental condition tested, i.e., of the reducing radical present ($NaHCO_2$ (N_2); $NaHCO_2$ (N_2O), 2-propanol (N_2) and 2-propanol (N_2O)). Furthermore, these two contributions (from now on labeled as Sp2 and Sp3) showed their main spectral features in the wavelength range associated with the lowest energy absorption band of the **RePtr** complex and therefore were ascribed to its reductive transformation, Sp2 being a transient species and Sp3 the stable product within the timescale of PR experiments. **Figure 9** compares the spectrum of the **RePtr** complex with the absolute spectra for the transient and the product calculated using the relative difference spectra resolved by MCR-ALS analysis, the radiation dose measured with the SCN^- actinometer and the radiation chemical yield of the 2-propanol radical.

In the PR reduction of free pterin solution either by e^-_{aq} or $CO_2^{\bullet-}$, several pterin radicals have been suggested as initial intermediates in the process of reduction. Since rapid protonation after the electron attack occurs, protonated (neutral) radicals at N8 or N3, and either the diprotonated (positive) radical at both N8 and N3 have been proposed [59],[60]. However, as the coordination to the metal undoubtedly should affect the relative basicity of the N atoms in the pterin ligand, we have used DFT and TDDFT calculations to support the proposed species for the transient intermediate observed in PR experiments. **Scheme I** shows the optimized structures of **RePtr**, of the protonated radicals at N8 (**RePtr(N8)$^\bullet$**) or N3 (**RePtr(N3)$^\bullet$**), as well as the optimized structure of the diprotonated radical at both N3 and N8 (**RePtr(N3,8)$^{\bullet+}$**), at the B3LYP/LanL2DZ/PCM (water) level of theory. **Figure 10** shows the calculated UV-vis absorption spectra for **RePtr**, **RePtr(N8)$^\bullet$, RePtr(N3)$^\bullet$, RePtr(N3,8)$^{\bullet+}$** and for the protonated reduced product $Re(CO)_3(7,8\text{-}PtrH_2)(H_2O)$ (**$RePtrH_2$,** see below). From the comparison of **Figures 9** and **10** it can be inferred that radical **RePtr(N8)$^\bullet$** seems to describe better than radical **RePtr(N3)$^\bullet$** the overall spectral features of differences Sp2. However, radical **RePtr(N3,8)$^{\bullet+}$** cannot be completely ruled out and radicals **RePtr(N8)$^\bullet$** and **RePtr(N3,8)$^{\bullet+}$** may both be contributing to the spectrum of Sp2.

The analysis of the concentration profiles obtained by MCR-ALS analysis suggested two consecutive processes for all the experimental conditions tested. The concentration profiles were adequately described by an initial first order process, followed by a second order reaction. Since the concentration of radicals initially produced by the pulse was

much lower than that of **RePtr**, the following kinetic model, eqs. 13 and 14, was proposed for the radiolysis experiments:

$$\mathbf{Sp1} + \mathbf{RePtr} \xrightarrow{k_1} \mathbf{Sp2} \qquad \mathbf{(13)}$$

$$\mathbf{2\ Sp2} \xrightarrow{k_2} \mathbf{Sp3} \qquad \mathbf{(14)}$$

Where **Sp1** stands for $\boldsymbol{e}^-_{aq}$, $CO_2^{\bullet-}$ or $(CH_3)_2C^{\bullet}OH$

Hence a Hard-Soft MCR-ALS model [34] was developed for improving the analysis of time resolved spectra. The model included a deterministic part, since the concentration profiles during the iterative procedure were simulated by using only two rate constants (k_1 and k_2) associated with the two consecutive steps.

Therefore, the computational model allowed obtaining not only the spectral shapes and the concentration profiles of each species involved, but also the optimal values for the rate constants associated with each reaction step. **Figure 11** compares the concentration profiles obtained by the HS-MCR-ALS model with the concentration profiles simulated using the optimal values for k_1 and k_2 for the experiment performed in the presence of 2-propanol and N_2O. Similar results were obtained for the other three experimental conditions tested. **Table 2** shows the optimal rate constant values obtained for the four experimental conditions tested.

Based on the what is known in the literature regarding pulse radiolytic, chemical and electrochemical reduction of free pterin [59]–[62] the reduction product **Sp3** can be proposed as the **$RePtrH_2$** complex. **Figure S10** shows the optimized structure of the **$RePtrH_2$** at the B3LYP/LanL2DZ/PCM (water) level of theory. The calculated spectrum of

RePtrH$_2$ reproduces with reasonable accuracy the resolved spectrum of **Sp3** of pulse radiolysis experiments (see **Figure 10**). Given that 7,8-PtrH$_2$ ligand is a two electrons reduction of pterin, a disproportionation reaction between two **RePtr(N8)•** radicals have to be invoked to account for the formation of **RePtrH$_2$,** eq. 15.

2 RePtr(N8)• $\rightarrow$ **RePtrH$_2$ + RePtr** **(15)**

This disproportionation reaction was proposed in the literature regarding reduction products of reduced pterin by PR [59],[60]. Disproportionation reactions of protonated reduced radicals of Re(I) complexes are common and well reported in the literature [35],[63]–[65].

Conclusions

The photochemical and thermal study realized in this work allowed us to identify the nature and characteristics of **RePtr** complex main excited states along with some intermediates and photo-products. In aqueous solutions, the complex luminescence is attributed to the emitting ^{1}IL state. In MeCN, however, both ^{1}IL and ^{3}MLCT states contribute to the complex luminescence, the latter state being deactivated by molecular oxygen. Flash photolysis experiments, either in aqueous or MeCN solutions, helped to identify the nature (^{1}IL and/or ^{3}MLCT) of the generated excited states. In glasses at 77K, nevertheless, the ^{3}MLCT prevailed over ^{1}IL states. TD-DFT calculations performed on the ligand and the complex are in good agreement with the fact that ϕ_{em} of **RePtr** is much

lower than that of the free ligand. The deactivation of ^{3}MLCT by O_2 leads to the formation of $^1O_2$ with a low quantum yield. No formation of $^1O_2$ in D_2O was detected, possibly due to a very low ^{3}IL formation quantum yield. When **RePtr** ^{3}MLCT is quenched by a sacrificial reductant, the species generated in flash photolysis experiments can be attributed to the radical of the reduced ligand. This intermediate was also observed in pulse radiolysis experiments. The stable product in the millisecond time scale could be assigned to the dihydrogenated complex $[Re(CO)_3(7,8\text{-}PtrH_2)(H_2O)]$. Under oxidative conditions a transient spectrum was obtained by pulse radiolysis which compares very well with those published for Re(II) species, suggesting that $N_3^{\bullet-}$ radical attack to the **RePtr** complex promotes the oxidation in the metal core.

Acknowledgements

This work was supported in part by CONICET (PIP 0389 and PIP 112-2013-01-00236CO), ANPCyT (PICT 2012-0423 and PICT 2015-0374) and UNLP (11X/611 and 11/X679) of Argentina. F. R. thanks CONICET for research scholarships. P.M. D.G. is a research member of CICBA (Argentina). F.S. G.E., E. W and G.T. R. are research members of CONICET (Argentina). Part of this work was also carried out in the Notre Dame Radiation Laboratory (NDRL). The NDRL is supported by the Division of Chemical Sciences, Geosciences and Biosciences, Basic Energy Sciences, Office of Science, United States Department of Energy through grant number DE-FC02-04ER15533. This is contribution number NDRL 5194.

References

[1] J. Berg, J. Tymoczko and L. Stryer, *Biochemistry, 5th edition*. 2002.

[2] S. Milstien, G. Kapatos, R.A. Levine, B. Shane, Chemistry and biology of pteridines and folates, National Institutes of Health, Bethesda, Maryland, 2001. doi:10.1016/0300-9084(94)90133-3.

[3] R.T. Parker, E. Freelander, S. Richard, E.M. Schulman, B. Dunlap, Room temperature phosphorescence of selected pteridines, Anal. Chem. 51 (1979) 1921–1926. doi:10.1039/an9901500155.

[4] C. Chahidi, M. Aubailly, Photophysical and photosensitizing properties of 2-amino-4 pteridinone: a natural pigment, Photochem. Photobiol. 33 (1981) 641–649. doi:10.1111/j.1751-1097.1981.tb05470.x.

[5] M.P. Denofrio, P.R. Ogilby, A.H. Thomas, C. Lorente, Selective quenching of triplet excited states of pteridines., Photochem. Photobiol. Sci. 13 (2014) 1058–1065. doi:10.1039/c4pp00079j.

[6] C. Lorente, A.H. Thomas, Photophysics and photochemistry of pterins in aqueous solution., Acc. Chem. Res. 39 (2006) 395–402. doi:10.1021/ar050151c.

[7] E. Wolcan, On the origins of the absorption spectroscopy of pterin and $Re(CO)_3$(pterin)(H_2O) aqueous solutions. A combined theoretical and experimental study., Spectrochim. Acta. A. Mol. Biomol. Spectrosc. 129 (2014) 173–183. doi:10.1016/j.saa.2014.03.022.

[8] A. Kumar, S. Sun, A.J. Lees, Photophysics and Photochemistry of Organometallic Rhenium Diimine Complexes, Top Organomet Chem. (2010) 1–35.

doi:10.1007/3418.

[9] M.A. Fox, Photoinduced electron transfer, Photochem. Photobiol. 52 (1990) 617–627. doi:10.1111/j.1751-1097.1990.tb01808.x.

[10] K. Kalyanasundaram, Photophysics, photochemistry and solar energy conversion with tris(bipyridyl)ruthenium(II) and its analogues, Coord. Chem. Rev. 46 (1982) 159–244. doi:10.1016/0010-8545(82)85003-0.

[11] K. Kalyanasundaram, M. Gratzel, Photosensitization and Photocatalysis Using Inorganic and Organometallic Compounds., SPRINGER-SCIENCE+BUSINESS MEDIA, B.V., Lausanne, Switzerland, 1993. doi:10.1017/CBO9781107415324.004.

[12] L. Sacksteder, M. Lee, Long-lived, highly luminescent rhenium (I) complexes as molecular probes: intra-and intermolecular excited-state interactions, J. Am. Chem. Soc. 115 (1993) 8230–8238. doi:10.1021/ja00071a036.

[13] M. Louie, T.T. Fong, K. Kam-, Luminescent Rhenium (I) Polypyridine Fluorous Complexes as New Biological Probes, Inorg. Chem. 50 (2011) 9465–9471. doi: 10.1021/ic201143f

[14] J.C. Calabrese, W. Tam, Organometallics for non-linear optics: Metal-pyridine and bipyridine complexes, Chem. Phys. Lett. 133 (1987) 244–245. doi:10.1016/0009-2614(87)87059-8.

[15] T.T. Ehler, N. Malmberg, K. Carron, B.P. Sullivan, L.J. Noe, Studies of Organometallic Self-Assembled Monolayers on Ag and Au Using Surface Plasmon Spectroscopy, J. Phys. Chem. 101 (1997) 3174–3180. doi:10.1021/jp963846r.

[16] B. Higgins, B. a DeGraff, J.N. Demas, Luminescent transition metal complexes as

sensors: structural effects on pH response., Inorg. Chem. 44 (2005) 6662–6669. doi:10.1021/ic050044e.

[17] Ting-Ting Meng, Hao Wang, Ze-Bao Zheng, and Ke-Zhi Wang, pH-Switchable "Off–On–Off" Near-Infrared Luminescence Based on a Dinuclear Ruthenium(II) Complex, Inorg. Chem. 56 (2017) 4775−4779. doi:10.1021/acs.inorgchem.7b00223.

[18] B.R. Spencer, B.J. Kraft, C.G. Hughes, M. Pink, J.M. Zaleski, Modulating the light switch by ^{3}MLCT-$^{3}\pi\pi^{*}$ state interconversion, Inorg. Chem. 49 (2010) 11333–11345. doi:10.1021/ic1011617.

[19] T. Biver, F. Secco, M. Venturini, Mechanistic aspects of the interaction of intercalating metal complexes with nucleic acids, Coord. Chem. Rev. 252 (2008) 1163–1177. doi:10.1016/j.ccr.2007.10.008.

[20] G.T. Ruiz, M.P. Juliarena, R.O. Lezna, E. Wolcan, M.R. Feliz, G. Ferraudi, Intercalation of *fac*-[(4,4'-bpy)Re^{I}(CO)$_3$(dppz)]$^{+}$, dppz = dipyridyl[3,2-a:2'3'-c]phenazine, in polynucleotides. On the UV-vis photophysics of the Re(I) intercalator and the redox reactions with pulse radiolysis-generated radicals., Dalton Trans. 3 (2007) 2020–2029. doi:10.1039/b614970g.

[21] S.B. Jimenez Pulido, M. Sieger, A. Kno, O. Heilmann, M. Wanner, B. Schwederski, J. Fiedler, M.N. Moreno Carretero, W. Kaim, Rhenium (I) coordinated lumazine and pterin derivatives : structure and spectroelectrochemistry of reversibly reducible (6-ATML)Re(CO)$_3$Cl (6-ATML = 6-acetyl-1,3,7-trimethyllumazine), Inorganica Chim. Acta. 325 (2001) 65–72. doi:10.1016/S0020-1693(01)00646-6.

[22] O. Heilmann, F.M. Hornung, J. Fiedler, W. Kaim, Organometallic iridium(III) and

rhenium(I) complexes with lumazine, alloxazine and pterin derivatives, J. Organomet. Chem. 589 (1999) 2–10. doi:10.1016/S0022-328X(99)00294-6.

[23] C. Bessenbacher, C. Vogler, W. Kaim, Stabilization of Biochemically Interesting Intermediates by Metal Coordination. 6. Charge Transfer in Complexes of 1,3-dimethyllumazine with Low-Valent Metals, Inorg. Chem. 28 (1989) 4645–4648. doi:10.1021/ic00325a021.

[24] S. Miyazaki, T. Kojima, J.M. Mayer, S. Fukuzumi, Proton-coupled electron transfer of ruthenium(III)-pterin complexes: a mechanistic insight., J. Am. Chem. Soc. 131 (2009) 11615–11624. doi:10.1021/ja904386r.

[25] F. Ragone, G.T. Ruiz, O.E. Piro, G.A. Echeverría, F.M. Cabrerizo, G. Petroselli, R. Erra-Balsells, K. Hiraoka, F.S. García Einschlag, E. Wolcan, Water-Soluble (Pterin)rhenium(I) Complex: Synthesis, Structural Characterization, and Two Reversible Protonation-Deprotonation Behavior in Aqueous Solutions, Eur. J. Inorg. Chem. 2012 (2012) 4801–4810. doi:10.1002/ejic.201200681.

[26] F. Ragone, H.H. Martínez Saavedra, P.F. García, E. Wolcan, G.A. Arguello, G.T. Ruiz, Association studies to transporting proteins of *fac*-$Re^{I}(CO)_3$(pterin)(H_2O) complex, J. Biol. Inorg. Chem. 3 (2016) 1–10. doi:10.1007/s00775-016-1410-7.

[27] A.H. Thomas, C. Lorente, A.L. Capparelli, M.R. Pokhrel, A.M. Braun, E. Oliveros, Fluorescence of pterin, 6-formylpterin, 6-carboxypterin and folic acid in aqueous solution: pH effects, Photochem. Photobiol. Sci. 1 (2002) 421–426. doi:10.1039/b202114e.

[28] F. Ragone, H.H. Martinez Saavedra, P.M. David Gara, G.T. Ruiz, E. Wolcan,

Photosensitized generation of singlet oxygen from Re(I) complexes: a photophysical study using LIOAS and luminescence techniques., J. Phys. Chem. A. 117 (2013) 4428–4435. doi:10.1021/jp402550g.

[29] P. Van Haver, L. Viaene, M. Van der Auweraer, F.C. De Schryver, References for laser-induced optoacustic spectroscopy using UV excitation, J. Photochem. Photobiol. A Chem. 63 (1992) 265–277. doi:10.1016/1010-6030(92)85192-W.

[30] S. Abbruzzetti, C. Viappiani, D.H. Murgida, R. Erra-Balsells, G.M. Bilmes, Non-toxic, water-soluble photocalorimetric reference compounds for UV and visible excitation, Chem. Phys. Lett. 304 (1999) 167–172. doi:10.1016/S0009-2614(99)00306-1.

[31] S.E. Braslavsky, G.E. Heibel, Time-Resolved Photothermal and Photoacoustic Methods Applied to Photoinduced Processes in Solution, Chem. Rev. 92 (1992) 1381–1410. doi**:** 10.1021/cr00014a007.

[32] R. Schmidt, C. Tanielian, R. Dunsbach, C. Wolff, Phenalenone, a universal reference compound for the determination of quantum yields of singlet oxygen $O_2(^1\Delta_g)$ sensitization, J. Photochem. Photobiol. A Chem. 79 (1994) 11–17. doi:10.1016/1010-6030(93)03746-4 .

[33] M.R. Feliz, G.J. Ferraudi, Double-pulse dichromatic photolysis of *fac*-$ClRe(CO)_3L_2$ (L = 4-phenylpyridine or 4-cyanopyridine): photohomolysis of Re-L bonds induced by irradiation of photochemically unreactive charge-transfer states, J. Phys. Chem. 96 (1982) 3059–3062. doi:10.1021/j100186a052.

[34] A. de Juan, R. Tauler, Multivariate Curve Resolution (MCR) from 2000: Progress in

Concepts and Applications, Crit. Rev. Anal. Chem. 36 (2006) 163–176. doi:10.1080/10408340600970005.

[35] L.B. Bracco, F.S. García Einschlag, E. Wolcan, G.J. Ferraudi, On the mechanism of the photoinduced reduction of an adduct of ferricytochrome C with a poly(4-vinylpyridine) polymer containing -$Re^{I}(CO)_3$(3,4,7,8-tetramethyl-1,10-phenanthroline) pendants, J. Photochem. Photobiol. A Chem. 208 (2009) 50–58. doi:10.1016/j.jphotochem.2009.08.003.

[36] G. V. Buxton, C.L. Greenstock, W.P. Helman, A.B. Ross, Critical review of rate constants for reactions of hidrated electrons, hidrogen atoms and hydroxyl radicals ($^{\bullet}$OH/$^{\bullet}$O-) in aqueous solution, J. Phisycal Chem. Ref. Data. 17 (1988) 513–886. doi:10.1063/1.555805.

[37] G. Hug, Y. Wang, C. Schöneich, Multiple time scales in pulse radiolysis. Application to bromide solutions and dipeptides, Radiat. Phys. Chem. 54 (1999) 559–566. doi:10.1016/S0969-806X(98)00303-X.

[38] P. Wardman, Reduction Potentials of One-Electron Couples Involving Free Radicals in Aqueous Solution, J. Phys. Chem. Ref. Data. 18 (1989) 1637–1755. doi:10.1063/1.555843.

[39] M. Feliz, G. Ferraudi, Charge-Transfer Processes in (4-Nitrobenzoate) $Re(CO)_3(azine)_2$ Complexes . Competitive Reductions of 4-Nitrobenzoate and Azine in Thermally and Photochemically Induced Redox Processes, Inorg. Chem. 37 (1998) 2806–2810. doi:10.1021/ic971241j.

[40] P. Hohenberg, W. Kohn, Inhomogeneous electron gas, Phys. Rev. 136 (1964) 1912–

1919. doi:10.1103/PhysRevB.7.1912.

[41] W. Kohn, L.J. Sham, Self-consistent equations including exchange and correlation effects, Phys. Rev. 140 (1965) A1133-A1138. doi:10.1103/PhysRev.140.A1133.

[42] R. Parr, W. Yang, Density-functional theory of atoms and molecules, Oxford University Press, New York, 1989.

[43] R. Bauernschmitt, R. Ahlrichs, Treatment of electronic excitations within the adiabatic approximation of time dependent density functional theory., Chem. Phys. Lett. 256 (1996) 454–464. doi:10.1016/0009-2614(96)00440-X.

[44] M.E. Casida, C. Jamorski, K.C. Casida, D.R. Salahub, Molecular excitation energies to high-lying bound states from time-dependentdensity- functionalresponsetheory: Characterizationand correctionofthetime-dependentlocal densityapproximation ionization threshold Mark, J. Chem. Phys. 108 (1998) 4439-4449. doi:10.1063/1.475855.

[45] R.E. Stratmann, G.E. Scuseria, M.J. Frisch, An efficient implementation of time-dependent density-functional theory for the calculation of excitation energies of large molecules, J. Chem. Phys. 109 (1998) 8218–8224. doi:10.1063/1.477483.

[46] N. O'Boyle, A. Tenderholt, K. Langner, Software News and Updates cclib: A Library for Package-Independent Computational Chemistry Algorithms, J. Comput. Chem. 29 (2008) 839–845. doi:10.1002/jcc.

[47] V. Barone, M. Cossi, Quantum calculation of molecular energies and energy gradients in solution by a conductor solvent model, J. Phys. Chem. A. 102 (1998) 1995–2001. doi:10.1021/jp9716997.

[48] M. Cossi, V. Barone, Time-dependent density functional theory for molecules in liquid solutions, J. Chem. Phys. 115 (2001) 4708–4717. doi:10.1063/1.1394921.

[49] B. Mennucci, J. Tomasi, Continuum solvation models: A new approach to the problem of solute s charge distribution and cavity boundaries, J. Chem. Phys. 106 (1997) 5151–5158. doi:10.1063/1.473558.

[50] D. Feller, The role of databases in support of computational chemistry calculations, J. Comput. Chem. 17 (1996) 1571–1586. doi:10.1002/(SICI)1096-987X(199610)17:13<1571::AID-JCC9>3.0.CO;2-P.

[51] K.L. Schuchardt, B.T. Didier, T. Elsethagen, L. Sun, V. Gurumoorthi, J. Chase, J. Li, T.L. Windus, Basis set exchange: A community database for computational sciences, J. Chem. Inf. Model. 47 (2007) 1045–1052. doi:10.1021/ci600510j.

[52] A. Serr, N. O'Boyle, GaussSum 2.2.5 program documentation, (2009).

[53] L. Helm, Ligand exchange and complex formation kinetics studied by NMR exemplified on *fac*-$[(CO)_3M(H_2O)]^+$ (M=Mn, Tc, Re), Coord. Chem. Rev. 252 (2008) 2346–2361. doi:10.1016/j.ccr.2008.01.009.

[54] R. Schmidt, The effect of solvent polarity on the balance between charge transfer and non-charge transfer pathways in the sensitization of singlet oxygen by pipi triplet states., J. Phys. Chem. A. 110 (2006) 5990–5997. doi:10.1021/jp060017p.

[55] R. Battino, T.R. Rettich, T. Tominaga, The solubility of oxygen and ozone in liquids, J. Phisycal Chem. 12 (1983) 163-178. doi:10.1063/1.555680.

[56] C. Martí, O. Jürgens, O. Cuenca, M. Casals, S. Nonell, Aromatic ketones as standards for singlet molecular oxygen photosensitization. Time-resolved photoacoustic and

near-IR emission studies, J. Photochem. Photobiol. A Chem. 97 (1996) 11–18. doi:10.1016/1010-6030(96)04321-3.

[57] M.P. Serrano, C. Lorente, C.D. Borsarelli, A.H. Thomas, Unraveling the Degradation Mechanism of Purine Nucleotides Photosensitized by Pterins: The Role of Charge-Transfer Steps, ChemPhysChem. 16 (2015) 2244–2252. doi:10.1002/cphc.201500219.

[58] G.T. Ruiz, M.P. Juliarena, E. Wolcan, G. Ferraudi, Kinetic and spectroscopic observations on the azidyl, , radical oxidation of *fac*-($L_{spectator}$)$Re^{I}(CO)_3$($L_{acceptor}$) to *fac*-($L_{spectator}$)$Re^{II}(CO)_3$($L_{acceptor}$), $L_{spectator}$=4,4′-bpy; $L_{acceptor}$=dipyridyl[3,2-a:2′3′-c]phenazine or $L_{spectator}$=Cl^-; $L_{acceptor}$=bathocup, Inorganica. Chim. Acta. 360 (2007) 3681–3687. doi:10.1016/j.ica.2007.02.049.

[59] P. Moorthy, E. Hayon, One-Electron Redox Reactions of Water-Soluble Vitamins. II. Pterin and Folic Acid, J. Org. Chem. 41 (1976) 1607–1613. doi:10.1017/CBO9781107415324.004..

[60] M. Farahank, P.S. Surdhar, S. Allen, D.A. Armstrong, M. Farahani, P.S. Surdhar, S. Allen, D.A. Armstrong, C. Sconeich, Y. Mao, A. Klaus-Dieter, M. Farahank, P.S. Surdhar, S. Allen, D.A. Armstrong, Reactions of $CO_2^{\bullet-}$ Radicals with Pterin and Pterin-6-carboxylate Ions, J. Am. Chem. Soc. Perkin Trans. 2. 2 (1991) 1687–1693. doi:10.1039/P29910001687.

[61] R. Raghavan, G. Dryhurst, Redox chemistry of reduced pterin species, J. Electroanal. Chem. 129 (1981) 189–212. doi:10.1016/S0022-0728(81)80014-9.

[62] S. Kwee, H. Lund, Electrochemistry of some substituted pteridines, BBA - Gen. Subj.

297 (1973) 285–296. doi:10.1016/0304-4165(73)90075-5.

[63] E. Wolcan, G. Ferraudi, Photochemical and Photophysical Properties of *Fac*-Re(I) Tricarbonyl Complexes: A Comparison of Monomer and Polymer Species with -$Re^{I}(CO)_3$Phen Chromophores, J. Phys. Chem. A. 104 (2000) 3–8. doi:10.1021/jp001135u.

[64] L.B. Bracco, R.O. Lezna, J. Muñoz-Zuñiga, G.T. Ruiz, M.R. Féliz, G.J. Ferraudi, F.S. García Einschlag, E. Wolcan, On the mechanism of formation and spectral properties of radical anions generated by the reduction of –[$Re^{I}(CO)_3$(5-nitro-1,10-phenanthroline)]$^{+}$ and –[$Re^{I}(CO)_3$(3,4,7,8-tetramethyl-1,10-phenanthroline)]$^{+}$ pendants in poly-4-vinylpyridine polymers, Inorganica. Chim. Acta. 370 (2011) 482–491. doi:10.1016/j.ica.2011.02.039.

[65] L.L.B. Bracco, M.R. Féliz, E. Wolcan, On the quenching of MLCT luminescence by amines: The effect of nanoaggregation in the decrease of the reorganization energy, J. Photochem. Photobiol. A Chem. 210 (2010) 23–30. doi:10.1016/j.jphotochem.2009.12.010.

Figure captions

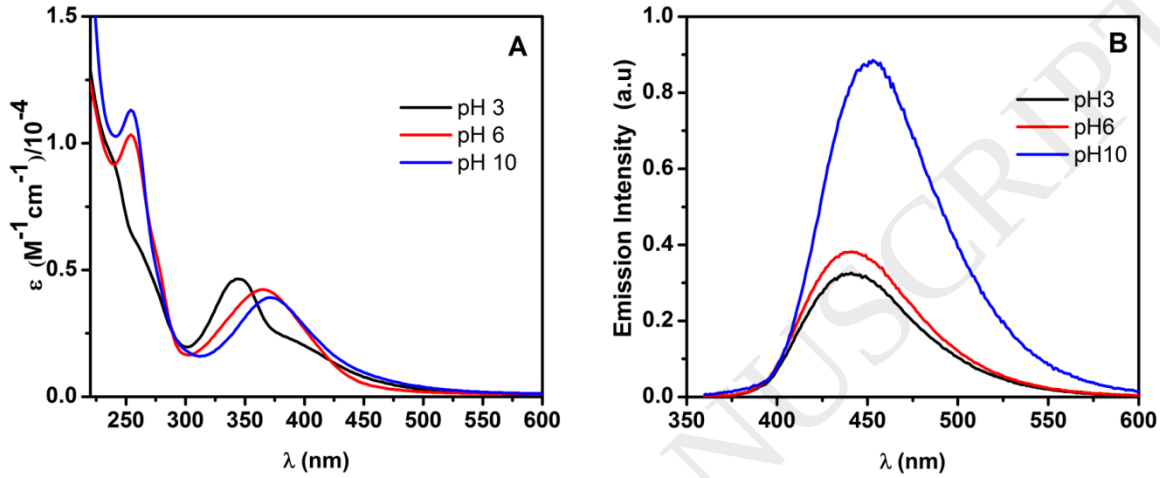

Fig. 1. (A) Absorption and **(B)** Emission spectra of the three forms acid base of the **RePtr** complex in aqueous solution at pH = 3, 6 and 10. λ_{exc} = 350 nm

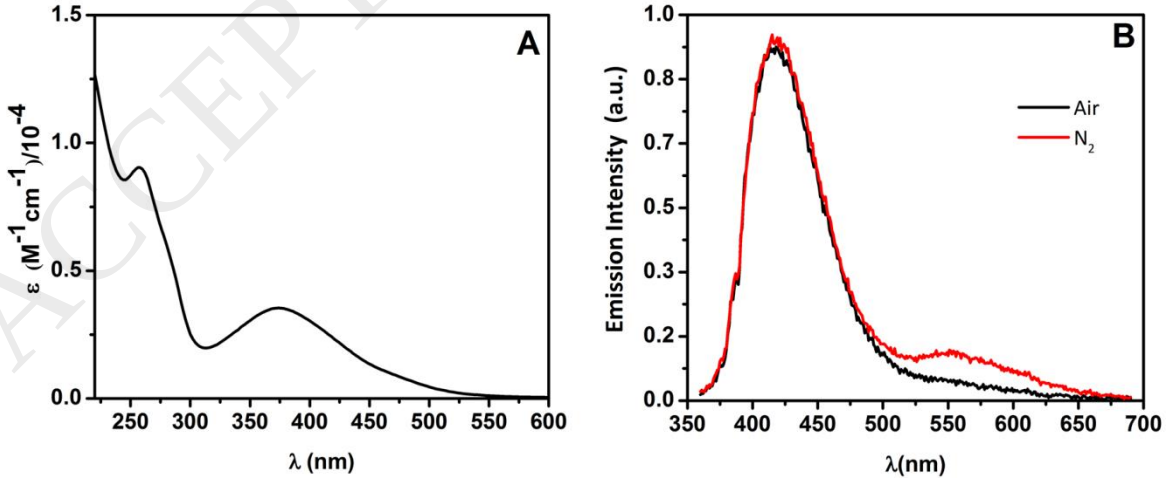

Fig. 2. (A) Absorption spectrum of the **RePtr** complex in deaerated MeCN and **(B)** emission spectra of the **RePtr** complex in deaerated and aerated MeCN solution. λ_{exc} = 350 nm

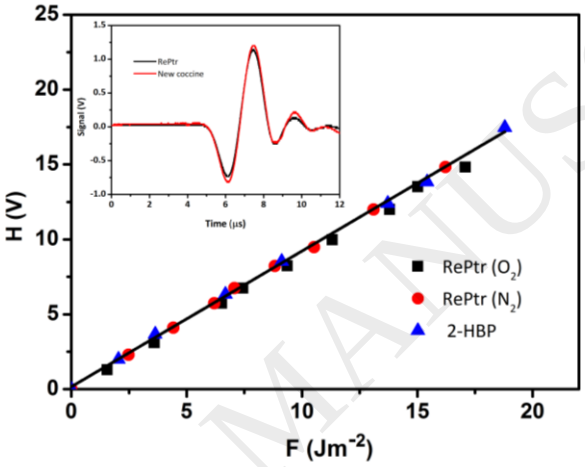

Fig. 3. Amplitude of the photoacoustic signals as a function of laser fluence for acetonitrile solutions: 2-hydroxybenzophenone (2-HBP) and **RePtr** complex (in N_2 and O_2). Inset: Normalized photoacoustic signals of aqueous solutions for New Coccine and the sample with matched absorbances (0.118 ± 0.002).

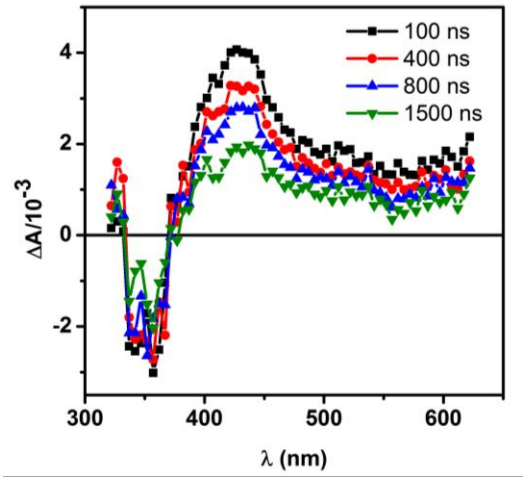

Fig. 4. Absorption spectra of the transient obtained in the λ_{exc} = 355 nm flash irradiation of the **RePtr** complex in a pH = 6 aqueous solution. Delays from the laser flash are reported in the figure.

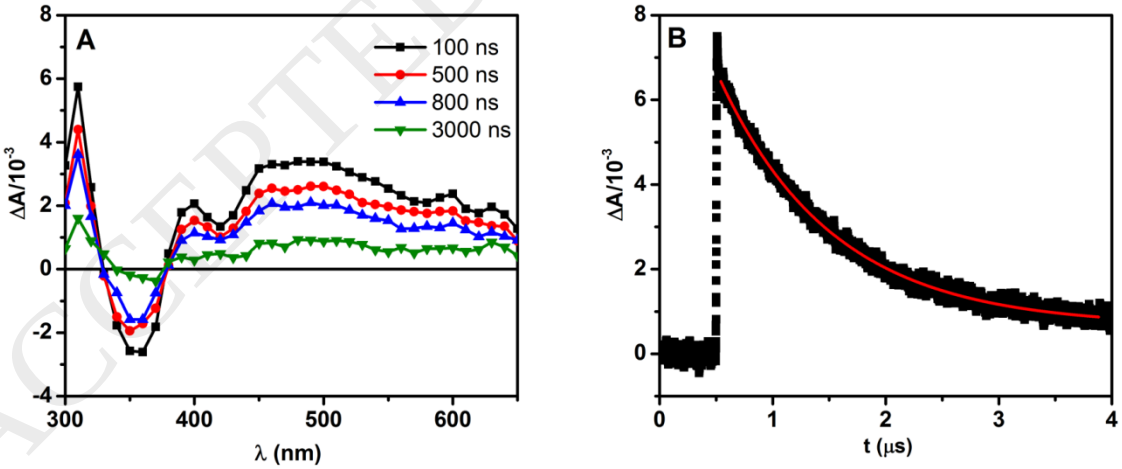

Fig. 5. (A) Absorption spectra of the **RePtr** complex transient in MeCN obtained by flash photolysis experiments at different times after pulse. λ_{exc} = 355 nm **(B)** Trace of the transient at λ_{obs} = 560 nm.

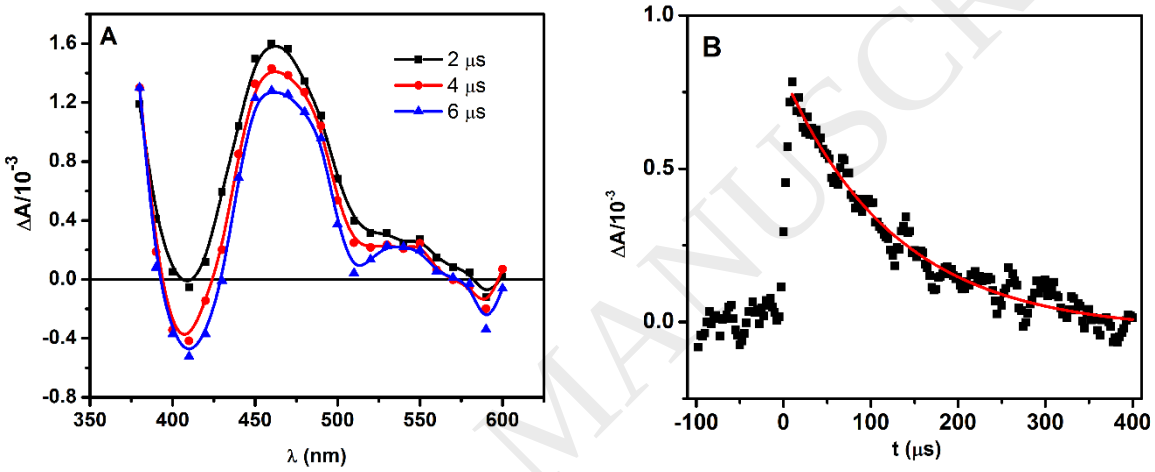

Fig. 6. (A) Absorption spectra of the **RePtr** complex transient in MeCN with TEA 0.1 M obtained by flash photolysis experiments at different times after pulse. λ_{exc} = 355 nm **(B)** Trace of the transient at λ_{obs} = 440 nm.

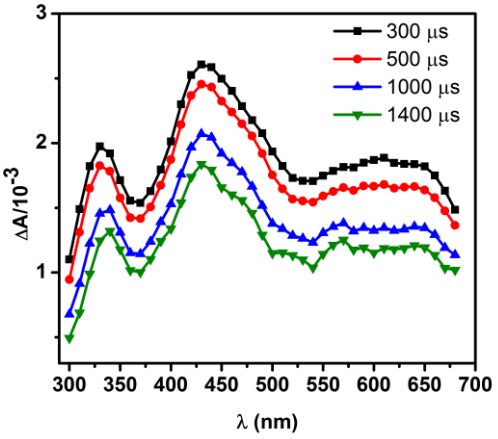

Fig. 7. Absorption spectra of **RePtr** complex oxidized by $N_3^{\bullet-}$ radical. (aqueous solutions, phosphate buffer pH 6, N_2O)

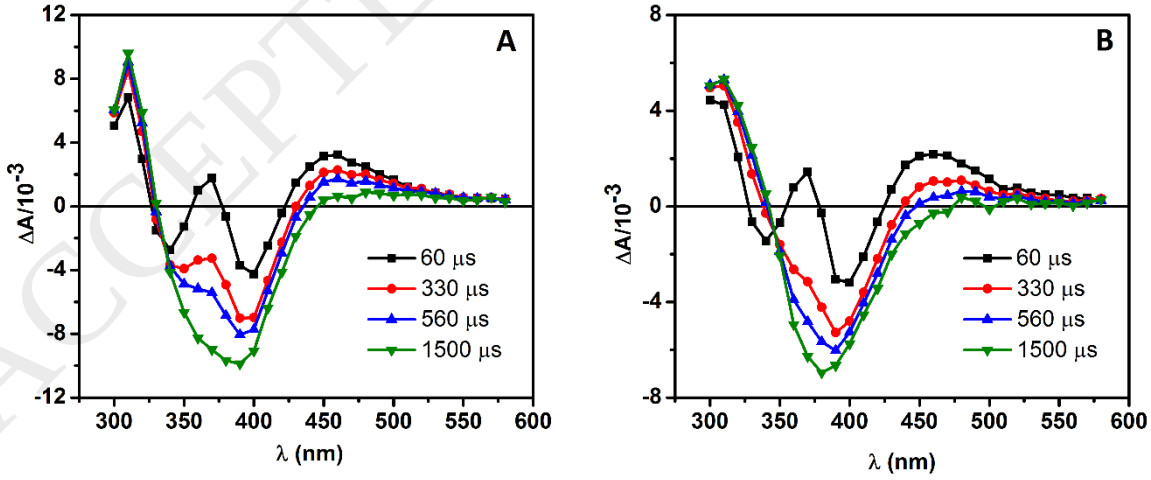

Fig. 8. Transients absorption spectra of the reduction of **RePtr** complex complex by **(A)** e^-_{aq} and **(B)** $CO_2^{\bullet-}$ (aqueous solutions, phosphate buffer pH = 6, $[Na(HCO_2)] = 10^{-2}$ M)

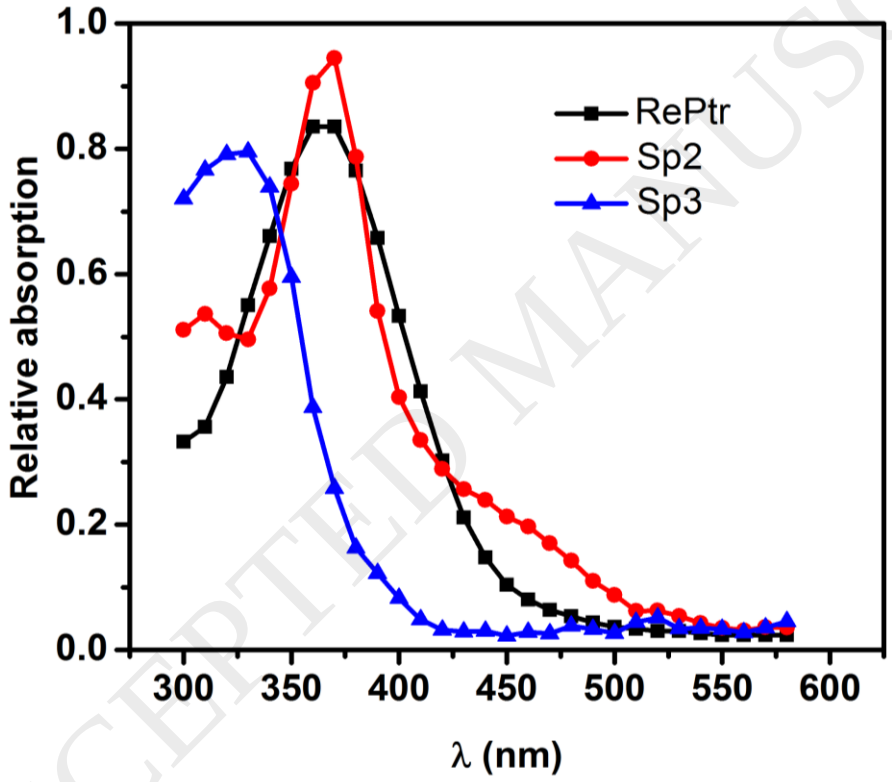

Fig. 9. Absolute spectra of **RePtr** complex, transient (Sp2) and product (Sp3), N_2O, pH = 6.

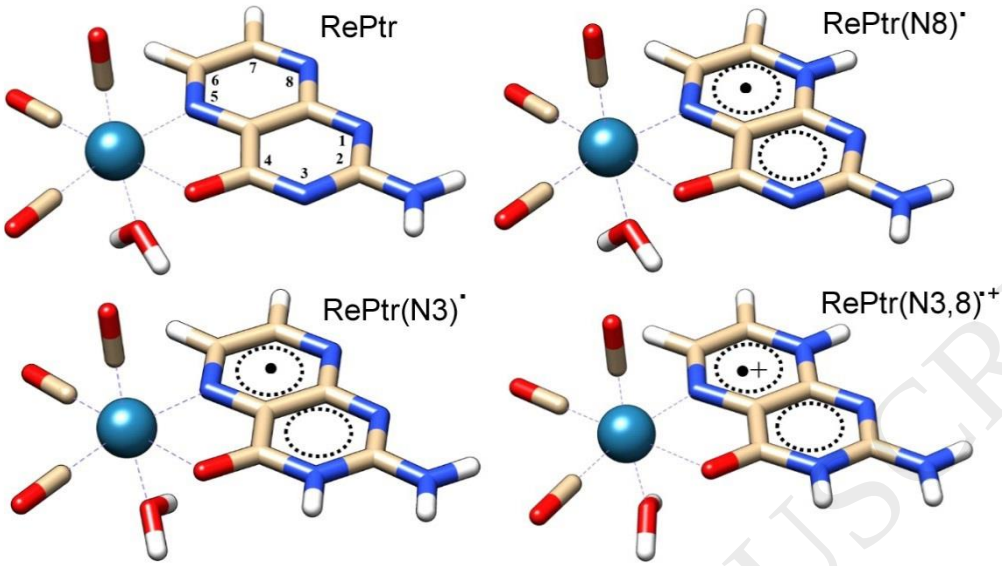

Fig. 10. Absorption spectra obtained by DFT and TDDFT calculations for the **RePtr** complex, the protonated radicals **RePtr(N8)•**; **RePtr(N3)•** and **RePtr(N3,8)•,** and **RePtrH$_2$**.

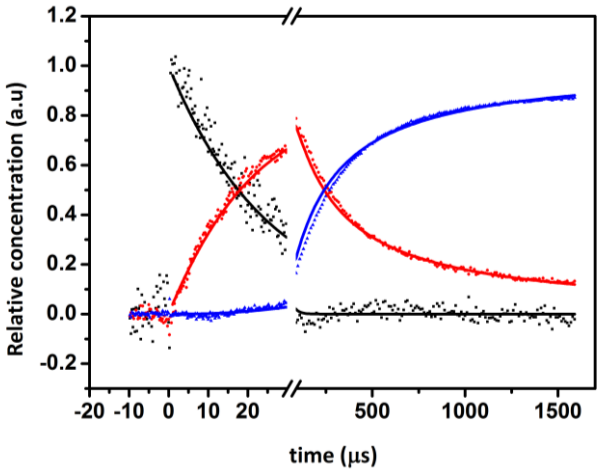

Fig. 11. HS-MCR-ALS concentration profiles and concentration profiles simulated of PR experiment (N_2 or N_2O).

Scheme I. Optimized structures of **RePtr**, of the protonated radicals at **RePtr(N8)$^{\bullet}$** and **RePtr(N3)$^{\bullet}$**, and diprotonated radical **RePtr(N3,8)$^{\bullet+}$**.

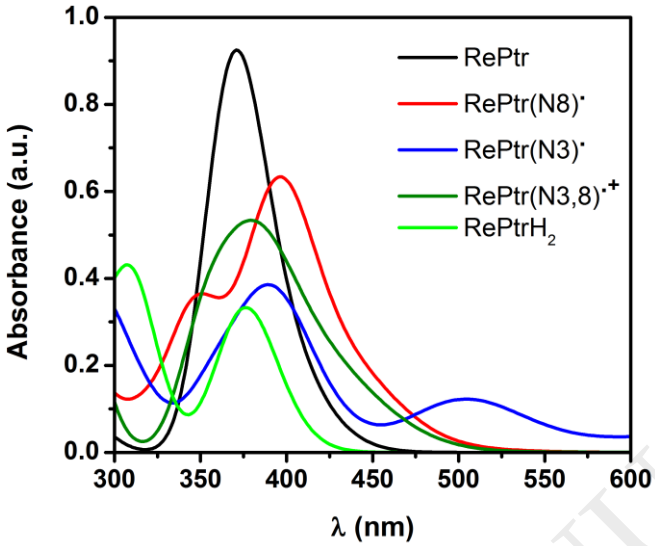

Solvent	λ_{max}(nm)	τ (N_2)/ns	τ (air)/ns	τ (O_2)/ns	$k_q/10^9 M^{-1}s^{-1}$	ϕ_{em}(air)(±10%)
H_2O						
pH = 3	441	7.7	7.4	7.4	--	6.4×10^{-2}
pH = 6	441	8.7	8.7	8.3	--	9.1×10^{-2}
pH = 10	454	6.9	6.6	6.6	--	2.5×10^{-1}
CH_3CN	418	8.0	8.0	--		1.7×10^{-2}
	565	8.0 1.0×10^3	8.0 2.8×10^2	-- 70	1.6	1.9×10^{-2} (N_2)

Table 1. RePtr luminescence properties: λ_{max}, lifetimes (λ_{exc} = 341 nm) and luminescence quantum yields in aqueous and acetonitrile solutions. Estimated lifetimes uncertainties are ± 5%.

	Gas	$NaHCO_2$	2-propanol
k_1 / s	N_2	3.67 (± 0.08) x 10^5	3.42 (± 0.07) x 10^5
	N_2O	3.70 (± 0.07) x 10^4	3.94 (± 0.05) x 10^4
k_2 / M.s	N_2	2.08 (± 0.04) x 10^8	2.59 (± 0.03) x 10^8
	N_2O	1.60 (± 0.03) x 10^8	4.34 (± 0.05) x 10^8

Table 2. Absolute rate constants obtained from a Hard-Soft MCR-ALS model applied to PR experiments carried out with **RePtr** complex under different experimental conditions. See text for details.